Observable imprints of primordial gravitational waves on the temperature anisotropies of the cosmic microwave background

Miguel-Angel Sanchis-Lozano* and Veronica Sanz†
Departamento de Física Teórica and Instituto de Física Corpuscular, CSIC-University of Valencia, 46100 Valencia, Spain

(Received 11 January 2024; accepted 28 February 2024; published 18 March 2024)

We examine the contribution of tensor modes, in addition to the dominant scalar ones, on the temperature anisotropies of the cosmic microwave background (CMB). To this end, we analyze in detail the temperature two-point angular correlation function $C(\theta)$ from the Planck 2018 dataset, focusing on large angles ($\theta \gtrsim 120°$) corresponding to small ℓ multipoles. A hierarchical set of infrared cutoffs are naturally introduced to the scalar and tensor power spectra of the CMB by invoking an extra Kaluza-Klein spatial dimension compactifying at about the grand unified theory scale between the Planck epoch and the start of inflation. We associate this set of lower scalar and tensor cutoffs with the parity of the multipole expansion of the $C(\theta)$ function. By fitting the Planck 2018 data we compute the multipole coefficients, thereby reproducing the well-known odd-parity preference in angular correlations seen by all three satellite missions: *Cosmic Background Explorer*, WMAP, and *Planck*. Our fits improve significantly once tensor modes are included in the analysis, hence providing a hint of the imprints of primordial gravitational waves on the temperature correlations observed in the CMB today. To conclude, we suggest a relationship between, on the one hand, the lack of (positive) large-angle correlations and the odd-parity dominance in the CMB and, on the other hand, the effect of primordial gravitational waves on the CMB temperature anisotropies.

DOI: 10.1103/PhysRevD.109.063529

I. INTRODUCTION

In an inflationary scenario, primordial energy density inhomogeneities, due to the unavoidable quantum fluctuations of the primordial field, are the seed of the primary temperature CMB anisotropies, as well as the large scale structure of our observable universe today. Usually, temperature anisotropies are mainly attributed to the scalar modes of the inflaton field, while tensor modes are expected to be subdominant, therefore hardly distinguishable from the former and besides its physical interpretation is not straightforward [1]. On the other hand, common wisdom usually states that polarization of the CMB remains as the main hope to detect primordial gravitational waves (PGWs) produced in the very early Universe [2], as only tensor—and not scalar—modes can produce B modes of polarization [3]. Note, however, that disentangling B modes of PGWs from other noncosmological sources (e.g., gravitational lensing) renders this method rather cumbersome so far. Nevertheless, future very-high-precision measurements of the CMB polarization [4–6] could uncover a PGW background in this way.

In this work, we include the expected small but maybe still observable effect of the tensor modes on the CMB temperature correlations, especially at large angles (low multipoles), in spite of the big uncertainties including the cosmic variance [7]. Use will be made of a parity statistic [8,9] to highlight the long-standing apparent odd-parity preference (i.e., power excess in odd multipoles and deficit in even multipoles) shown by data of all three satellite missions—*Cosmic Background Explorer* (COBE) [10], WMAP [11], and *Planck* [12,13]—in the multipole analysis of the two-point correlation function. Notice that such a parity imbalance, even to a small degree, questions the large-scale isotropy of the observable Universe stemming from the cosmological principle.

In fact, the standard cosmological model can be viewed as a phenomenological effective theory of an unknown underlying more general theory yet to be discovered. Discrepancies, anomalies, or puzzles, which are emerging from observations with respect to a standard cosmology scenario [14–18], may have a systematic origin or can be due to statistical fluctuations. Their persistence, however, along different probes, implying uncorrelated errors, strongly suggest the need for new physics beyond the minimal Standard Model in cosmology and elementary particle physics. In this paper we will consider a cosmological (and common) origin to the lack of large-angle positive correlation and the dominance of the odd multipoles over the even ones at low ℓ.

*miguel.angel.sanchis@ific.uv.es
†veronica.sanz@uv.es

A. Angular correlations of the CMB and the Sachs-Wolfe effect

Two categories of temperature fluctuations observed in the CMB can be distinguished according to the cosmic time evolution: (a) primary anisotropies, prior to decoupling, and (b) secondary anisotropies, developing as photons propagate from the surface of the last scattering to the observer (us). The former include temperature fluctuations due to photon propagation under metric perturbations originated by inhomogeneities of the matter field at the time of recombination, the so-called Sachs-Wolfe (SW) effect. This effect shows up at rather large angles from directions in the celestial sphere, while secondary anisotropies (as well as baryonic acoustic oscillations) rather affect quite small angles and have been successfully accounted for by standard cosmology.

The SW effect will play an important role in our study to account for the temperature angular distribution, showing a lack of (positive) correlations at large angle (i.e., $\theta \gtrsim 60°$) together with an apparent parity imbalance. Usually, under some simplifying assumptions, a plateau is expected from this effect in the angular power spectrum at low ℓ ($\lesssim 30$), while a sawtooth shape favoring odd-ℓ peaks is actually observed, later interpreted in this paper.

B. Parity imbalance seen in the CMB

As is well known, nature is parity violating, e.g., in the electroweak sector of the Standard Model where only left-handed fermions are active [19]. In this context, it is natural to ask whether nature would again violate parity through some gravitational processes, and if this feature could shed light on the very early Universe itself. In fact, a variety of sources of gravitational parity violation have been considered in the literature, see, e.g., Refs. [20–23]. Any of these could have left an imprint on the net helicity of the gravity wave background, namely the preferred excitation of one circular polarization over another.

In the present study we follow the path, started in a previous paper (see Ref. [24]), where a certain degree of parity breaking showing up in correlations at large angle in the CMB radiation was envisaged. To this end, fundamental fermionic fields (making up a composite scalar inflaton) were introduced, satisfying periodic and antiperiodic conditions on a Hubble radius in real space. In this way, two distinct infrared cutoffs, associated with integer and half-integer Fourier modes of the fluctuating field, emerged as a source of parity breaking in angular correlations. In particular, a preference for odd multipoles at large angle comes out naturally in angular two-point correlations (see Appendix).

In this paper, however, we will not resort to fermionic fields as fundamental components of a composite scalar inflaton field to provide the required periodic and antiperiodic conditions, as done in Ref. [24]. Rather, we shall assume that in the very early Universe a preinflationary scalar field satisfies certain boundary conditions on an extra spatial dimension *à* la Kaluza-Klein (just one for simplicity), to be addressed in more detail in Sec. IV. Thereby, distinct comoving scales for infrared cutoffs (commonly related to the inverse radius of an extra dimension compactified as a circle) come into play in temperature angular correlations, modifying the scalar and tensor power spectra.

The scalar power spectrum is usually parametrized as

$$P^S(k) = A^S \left[\frac{k}{k_*}\right]^{n_s - 1}, \qquad (1)$$

where n_s is the scalar spectral index and k_* is the pivot scale. The above spectrum, referred exclusively to scalar modes, would be perfectly scale-free (i.e., $n_s = 1$) if the Hubble parameter $H_{\rm inf}$ were strictly constant during inflation. If $H_{\rm inf}$ evolves slowly, a slight deviation of the spectral index from unity is expected, and indeed the observations show that $n_s = 0.9649 \pm 0.0042$ [25].

A near scale-free $P^S(k)$ would have been generated as modes with comoving wave numbers k successively crossed the Hubble radius and classicalized, later reentering into the Hubble horizon of the observable Universe once inflation ended. Usually, no lower limit is assumed in the $P^S(k)$ spectrum so that in numerical computations of observables the integration range over Fourier modes is taken between zero and infinity.

On the other hand, a tensor power spectrum $P^T(k)$ is usually parametrized as

$$P^T(k) = A^T \left[\frac{k}{k_*}\right]^{n_T}, \qquad (2)$$

where the tensor spectral index n_T is expected to be negative and small but not vanishing.

From Eqs. (1) and (2), the tensor-to-scalar ratio r is defined as

$$r = \frac{A^T}{A^S} = \frac{P^T(k_*)}{P^S(k_*)}. \qquad (3)$$

Current limits on r severely constrain many models of inflation and we will later check that the tensor contributions computed in this work comply with such constraints.

II. TWO-POINT ANGULAR CORRELATION FUNCTION OF THE CMB

All three COBE, WMAP, and *Planck* satellite missions have observed that the temperature angular distribution of the CMB is remarkably homogeneous across the sky, with anisotropies of order 1 part in 10^5. This observation is, in fact, one of the main arguments in favor of an inflationary scenario in cosmology to solve the so-called horizon problem, together with the flatness and monopole problems [26].

A powerful test of these fluctuations relies on the two-point angular correlation function $C(\theta)$,[1] defined as the ensemble product of the temperature differences with respect to the average temperature T_0 from all pairs of directions in the sky defined by unitary vectors $\vec{n}_1$ and $\vec{n}_2$,

$$C(\theta) = \left\langle \frac{\delta T(\vec{n}_1)}{T_0} \frac{\delta T(\vec{n}_2)}{T_0} \right\rangle, \tag{4}$$

where $\theta \in [0, \pi]$ is the angle defined by the scalar product $\vec{n}_1 \cdot \vec{n}_2$.

The information contained in the angular power spectrum of the CMB is basically the same as in the correlation function, but the latter highlights the behavior at large angles (small ℓ) where a sizable disagreement between theoretical expectations and observations has been found (see, e.g., Refs. [29–32]). In this work, we focus on the analysis of angular correlations, searching specifically for imprints from the very early Universe on the temperature fluctuations.

The temperature two-point correlation function is usually expanded as

$$C(\theta) = \sum_{\ell \geq 2} \frac{(2\ell+1)}{4\pi} C_\ell P_\ell(\theta), \tag{5}$$

where $P_\ell(\theta)$ is the order-ℓ Legendre polynomial, and the sum extends from $\ell = 2$ since the monopole and dipole contributions have been removed from the analysis.

In the following, we will ignore the transfer function and consider only the SW effect as the main source of primary anisotropies, as expected on scales larger than $\simeq 1°$. Hence, the multipole coefficients of Eq. (5) can be computed in the limit of a flat power spectrum $P^S(k)$, as

$$C_\ell^S = \frac{2N^S}{\pi} \int_0^\infty du \frac{j_\ell^2(u)}{u} = \frac{N^S}{\pi \ell(\ell+1)}, \tag{6}$$

where j_ℓ is the spherical ℓ-Bessel function and N^S stands for a normalization factor [related to the amplitude A^S in Eq. (1)] to be determined from the fit to observational data.

An overall agreement between the behavior of $C(\theta)$ and observational points can be achieved if the C_ℓ coefficients comply with the SW plateau condition [$C_\ell \sim 1/\ell(\ell+1)$ at small ℓ]. However, the $\chi^2_{\mathrm{d.o.f.}}$[2] resulting from the fit turns out to be quite unsatisfactory (see Fig. 1) as, e.g., positive correlations arise at large angle, in contrast to the observed lack of large-angle correlations for $\theta \gtrsim 60°$–$70°$ [14], among other anomalies [33].

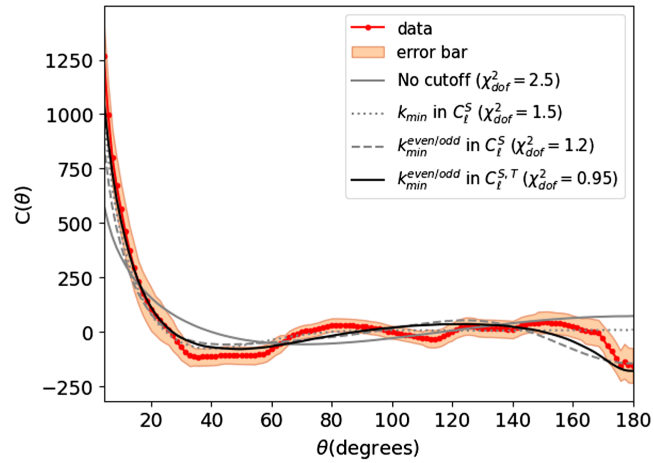

FIG. 1. Temperature two-point angular correlation function as a function of θ from the fit to Planck 2018 data, for the four different assumptions discussed in the text. The shadowed area represents one σ error bar.

III. SINGLE INFRARED CUTOFF IN THE SCALAR POWER SPECTRA

In order to improve the above-mentioned unsatisfactory fit, an infrared cutoff k_{min} was introduced *ad hoc* to the CMB power scalar spectrum in Ref. [34], implying a lower limit u_{min} in the integral of the multipole C_ℓ coefficients in Eq. (6),

$$C_\ell^S = \frac{2N^S}{\pi} \int_{u_{\mathrm{min}}}^\infty du \frac{j_\ell^2(u)}{u}, \tag{7}$$

where $k_{\mathrm{min}} = u_{\mathrm{min}}/r_d$ and r_d denotes the comoving distance to the last scattering surface. The authors of Ref. [34] introduced the infrared cutoff essentially in a heuristic way, whose purpose was removing the unseen (positive) correlations at large scale expected in standard cosmology. Later, a theoretical interpretation of k_{min} was given as the first oscillation mode to leave the Planck domain [35] within a linearly expanding (without inflation) universe (see [36]).

In Ref. [37], this study was consistently extended, focusing on the low-ℓ region of the power spectrum itself, providing an infrared cutoff value compatible with [34]. Furthermore, in Ref. [38] a suggestive connection between the lack of correlation at large angles provided by k_{min} and the odd-parity preference was shown. Indeed, the observed downward tail of the $C(\theta)$ function at large angles ($\theta \gtrsim 120°$) was nicely reproduced while keeping the good behavior of $C(\theta)$ over the whole examined angular range, i.e., $4° < \theta \leq 180°$.

[1] See also Refs. [27,28] for a discussion on higher-order correlation functions.

[2] Here we apply the statistical test $\chi^2_{\mathrm{d.o.f.}}$, which is used very often in particle physics analyses; see, e.g., the Particle Data Group review [25] for more details. Note that a good description of the data would correspond to a Pearson χ^2 distribution with a mean close to the number of degrees of freedom (d.o.f.), namely we aim for $\chi^2_{\mathrm{d.o.f.}} \simeq 1$, together with a good p-value.

Notice, however, that a heuristic tuning of the multipole coefficients ($\ell \lesssim 10$) was required in Ref. [38] in order to reach a good agreement with data. In a following work [24], *two* infrared cutoffs (instead of one) were set in the scalar power spectrum, providing the observed odd-parity preference of $C(\theta)$ but avoiding so many fit parameters.

Indeed, based on causality arguments, two maximum correlation lengths ($\lambda_{\rm max}^{\rm even}$ and $\lambda_{\rm max}^{\rm odd}$ affecting even- and odd-parity multipoles, respectively) were put forward in Ref. [24] in correspondence with two different boundary conditions. Then two comoving wave numbers ($k_{\rm min}^{\rm even}$ and $k_{\rm min}^{\rm odd}$) were defined accordingly for even- and odd-parity modes. The existence of such a doublet of (periodic and antiperiodic) boundary conditions was attributed to fundamental fermionic fields making up a composite inflaton [39].

Although following essentially this idea, no fermionic fields will be invoked in the present paper to get two different energy scales for the cutoffs. Rather, we will rely on a Kaluza-Klein (KK) model with an extra spatial dimension, so that appropriate boundary conditions of a scalar field (at the very early Universe) would yield even and odd fields (regarding their Fourier expansion in k modes) in the observable four-dimensional universe. Moreover, a similar pattern will be assumed for tensor fluctuations contributing to the angular correlation function, to be incorporated to our analysis as a second step.

First, let us examine a simple extra dimension model providing a theoretical framework and motivation for the phenomenological assumptions made so far, to be further developed in the subsequent sections.

IV. MODEL SETUP IN EXTRA DIMENSIONS

In this section we provide a specific scenario where those cutoffs would arise naturally. We will build a model in five dimensions (5D) of spacetime, which would lead to a 4D low-energy theory when the fifth dimension is compactified. This compactification would lead to the appearance of 4D Kaluza-Klein modes whose spectrum would dictate the cutoffs we mentioned.

Let us assume that nature at some high scale is five dimensional (5D). For simplicity, let us also assume for the moment that there is no curvature and those 5D are flat. This situation would be described by a 5D Minkowski metric

$$ds^2 = dt^2 - dx_i dx^i - dz^2, \tag{8}$$

where $i = 1$, 2, and 3, and we denote with z the fifth dimension. The Universe appears to be 4D, though, and very precise tabletop experiments do confirm that the gravitational attraction between two objects of masses m_1 and m_2 is the one expected from Newton's gravity in 4D, namely $V(r) \propto m/r$.

However, if gravity acted over a larger number of spacetime dimensions ($d = 4 + n$), the law would be modified to

$$V(r) = \frac{G_N m}{r^{1+n}},$$

where G_N would be Newton's strength in $n + 4$ dimensions. Assuming the n extra dimensions get compactified, the previous expression would change into a 4D Newton law modified by a volume factor that depends on the shape and size of the n extra dimensions. Current experiments place a limit on the size of flat compactified extra dimensions of a few tenths of micrometers, see Ref. [40] for a recent and most precise limit.

Tiny extra dimensions can arise through a process called compactification. There are various options to realize the compactification mechanism, including the presence of fluxes in Calabi-Yau manifolds. Depending on the configuration of the geometry and the fluxes, one can end up with different possibilities for a compact extra dimension.

For simplicity, let us assume that the extra dimension is simply a segment of size L. Fields propagating in this geometry could be factorized in the so-called KK decomposition. For any field, one can write their expression as follows:

$$\Phi(x^\mu, z) = \phi(x^\mu) f(z),$$

where x^μ, with $\mu = 0\ldots3$, are the 4D coordinates and z is the fifth dimension, $z \in [0, L]$.

For a scalar/fermion field in extra dimensions, their 4D fields $\phi(x^\mu)$ would satisfy the Klein-Gordon/Dirac equation of motion and the fifth component $f(z)$ would satisfy a wave function equation, which depends on the geometry and boundary conditions at the two extremes of the interval. For example, the field Φ could have Neumann or Dirichlet boundary conditions, namely

$$\begin{aligned} \partial_z \Phi|_{z=z_0} &= 0 \quad (\text{Neumann, or } +), \\ \Phi(z_0) &= 0 \quad (\text{Dirichlet, or } -). \end{aligned} \tag{9}$$

Those boundary conditions can be imposed in both extremes of the interval, at $z_0 = l_0$ and $z_0 = l_1$, leading to different options for fields in the extra dimension. From the 4D standpoint, these fields would appear as an infinite tower of 4D fields (KK tower) with masses determined by the boundary conditions.

Fields with Neumann boundary conditions at both ends ($z = l_0, z = l_1$) would be called $(+,+)$ and would exhibit a massless zero mode. Fields with other boundary conditions, $(\pm, \mp)$ and $(-,-)$, would have a KK spectrum with a lowest KK state ($n = 0$) with a nonzero mass, providing an IR cutoff in their spectrum. Those four options for boundary conditions at $z = l_0$ and l_1 have different properties under the parity $z \to -z$. Indeed,

$$(+,+) \text{ and } (-,-) \text{ are even, and } (+,-) \text{ and } (-,+) \text{ are odd.} \quad (10)$$

In flat geometries like the one described by the metric in Eq. (8), the mass spectrum of fields with boundary conditions $(+,-)$ and $(-,-)$ would be related as follows: $\frac{m_n^{(-,-)}}{m_n^{(+,-)}} = \frac{2n+2}{2n+1}$, where $n = 0, 1, \ldots$. For these 5D fields, the lowest mass in their spectrum ($n = 0$) provides a natural IR cutoff for their physical behavior. The IR cutoffs could be represented by a letter k_S and related by a simple factor 2,

$$\frac{k_S^{\text{even}}}{k_S^{\text{odd}}} = 2, \quad (11)$$

precisely the factor we would consider when evaluating their impact on the scalar two-point correlation in the CMB. Here we have labeled the field with $(-,-)$ as even and $(+,-)$ as odd, following the convention in the next sections. We have also added the subscript S to indicate the field we consider is scalar.

In addition to scalar or fermion fields, spin-two fields are unavoidably present in any spacetime geometry. From the 4D standpoint, the KK tower of the graviton spin-two field must contain a massless state, responsible for 4D gravity, and a tower of massive fields (KK gravitons) with the same quantum numbers as the massless graviton.

The condition of a massless state implies that the tensor field satisfies $(+,+)$ boundary conditions. This choice determines the rest of the graviton spectrum. The massive spin-two fields would follow a 4D Fierz-Pauli Lagrangian (describing a massive spin-two state) and their interactions with other species would be driven by the coupling to the stress tensor [41].

This construction can be generalized to metrics with curvature in the extra dimension. Those geometries, which we will call "warped," have been employed in various applications, including the AdS/CFT correspondence [42], in holographic approaches for QCD [43], for superconductivity [44], and for electroweak interactions [45,46]. Also, let us mention that successful inflation could be achieved in these kinds of scenarios by assuming the inflaton is a pseudo-Goldstone boson and its potential is generated by the KK contributions of fields in the extra dimension [47].

Warped geometries can be parametrized in terms of a warp factor $w(z)$ to represent classes of geometries given by a factorizable metric,

$$ds^2 = w(z)^2 (dt^2 - dx_i dx^i - dz^2), \quad (12)$$

where the case $w(z) = 1/(kz)$ would correspond to the anti–de Sitter (AdS) case, but other metrics like the Sakai-Sugimoto [48], $w(z) = 1/z^3$, Hirn-Sanz [43,49], $w(z) = e^{-c_d (z/l_1)^d}/z$, or the AdS-dilaton [50], $w(z) = e^{-z^2/2}/z$, have been employed in different physical situations.

In those cases, exact analytic expressions of the KK spectrum cannot be obtained, but in Ref. [51] closed expressions for the overall IR behavior of the spectrum (sum rules) were derived. In particular, a useful sum rule allows us to obtain the behavior of the even and odd KK towers in warped extra dimensions,

$$\frac{k_S^{\text{even}}}{k_S^{\text{odd}}} \simeq \frac{\int_{l_0}^{l_1} w(z)\alpha(z) dz \int_z^{l_1} dz'/w(z')}{\int_{l_0}^{l_1} w(z)\alpha(z) dz \int_{l_0}^{z} dz'/w(z')}, \quad (13)$$

where $\alpha(z) = \frac{\int_z^{l_1} dz'/w(z')}{\int_{l_0}^{l_1} dz'/w(z')}$, see [51] for more details. Using this sum rule, we recover the relation in Eq. (11) for the flat metric case, $w(z) = 1$.

Moreover, the relation (11) is more general and approximately holds for warped metrics. For example, in the AdS metric, the KK spectrum will be given by the zeros of complicated combinations of Bessel functions, see, e.g., Ref. [52]. Nonetheless, one can examine the asymptotic behavior of these relations when $m_n \gg k e^{-\pi k l_1}$, where the Bessel functions approximate to sine and cosine and many terms drop out. In this approximation, the KK spectrum can be understood by a simple set of relations,

$$\cos\left(\frac{m_n}{k e^{-k\pi l_1}}\right) \approx 0 \quad \text{for odd boundary conditions, and}$$
$$\sin\left(\frac{m_n}{k e^{-k\pi l_1}}\right) \approx 0 \quad \text{for even boundary conditions,} \quad (14)$$

which leads to the same approximate behavior of the lowest modes ($n = 0$) as in the flat extra-dimensional case, namely

$$\frac{k_S^{\text{even}}}{k_S^{\text{odd}}} \simeq 2 \quad \text{for warped metrics.} \quad (15)$$

Moreover, one can relate the KK tower of spin-two fields, KK gravitons, to other fields (fermions or scalars) propagating in the extra dimension. In flat geometries, the first KK graviton [coming from a $(+,+)$ field] would have its mass at the same value as the $(+,-)$ lowest mode of a scalar or fermion field, although this relation can be modified in the presence of curvature, typically leading to $k_T > k_S^{\text{odd}}$, as explained in Refs. [41,53].

The second KK-graviton state could also contribute to the tensor correlations. The mass would be double the first KK graviton, leading to a relation for the first two states in the KK-graviton spectrum $k_T' \simeq 2k_T$.

To summarize, fields propagating in an extra dimension exhibit a 4D spectrum that depends on the geometry and the boundary conditions. The impact of these fields on 4D observables can be computed as a sum over contributions of 4D Kaluza-Klein fields. Below the compactification scale, those contributions would be dominated by the lowest KK modes, whose masses provide a natural IR cutoff. In the analysis of the CMB spectrum, we will consider that the cutoffs coming from the extra-dimensional scenario would be as follows:

$$\text{Scalar cutoffs:}\ k_S^{\text{even}} = 2k_S^{\text{odd}}, \tag{16}$$

$$\text{Tensor cutoffs (from KK gravitons):}\ k_T \gtrsim k_S^{\text{odd}} \quad \text{and} \quad k'_T = 2k_T. \tag{17}$$

The scale hierarchy derived from these (infrared) cutoffs will be taken into account in the next sections when computing the respective correlation functions for scalar and tensor perturbations.

V. DOUBLE INFRARED CUTOFF IN THE SCALAR POWER SPECTRUM

Once provided a theoretical support to the appearance of a set of infrared cutoffs in the power spectra, let us employ the same notation as in Ref. [24] for the scalar case,

$$k_{\text{min}}^{\text{odd/even}} = \frac{u_{\text{min}}^{\text{odd/even}}}{r_d}, \tag{18}$$

corresponding to two lower cutoffs (instead of one) applying to the integral of Eq. (17), yielding

$$C^S_{\ell_{\text{odd/even}}} = \frac{2N^S}{\pi}\int_{u_{\text{min}}^{\text{odd/even}}}^{\infty} du\frac{j_\ell^2(u)}{u}, \tag{19}$$

where the lower limit of the integral is now $u_{\text{min}}^{\text{odd/even}} = k_{\text{min}}^{\text{odd/even}}/r_d$, thereby affecting differently the numerical values of the odd and even coefficients (actually only for low ℓ), therefore altering the shape of $C(\theta)$.

From a best fit of $C(\theta)$ to the Planck 2018 data, the following values for the lower cutoffs were obtained in Ref. [24]: $u_{\text{min}}^{\text{odd}} = 2.67 \pm 0.31$ and $u_{\text{min}}^{\text{even}} = 5.34 \pm 0.62$. In this work, we will recompute these lower cutoffs but incorporating tensor modes in our analysis, also imposing the relations from the compact extra dimension in Eq. (16). The new numerical values for the lower cutoffs do not differ greatly from the previous ones, but tensor fluctuations will certainly contribute to angular correlations, as we shall see soon.

Let us remark by now that the improvement regarding the parity dominance [affecting the downward tail in $C(\theta)$ at large angles] resulting from the introduction of two infrared cutoffs with respect to a single one is rather limited because the net effect is restricted to the first few multipoles: $\ell \lesssim u_{\text{min}}$. Let us mention in this regard the so-called ellipsoidal universe [54–56], where only the quadrupole term is actually modified, however, yielding a noticeable effect at large angular scale.

To overcome this drawback and extend the influence of the lower cutoff(s) on the multipole expansion of $C(\theta)$, we will next include the contribution of tensor modes, thereby modifying further and reaching higher C_ℓ coefficients.

VI. TENSOR MODES AND EXTRA INFRARED CUTOFFS

In this section we address the effect of primordial gravity waves generated during inflation on the CMB temperature anisotropies due to tensor modes, which constitutes the main goal of this paper. To this end, and taking into account that we are examining angular correlations, the following expression will be used to compute the tensor coefficient of the ℓ multipole according to Ref. [57]:

$$\begin{aligned} C_\ell^T &= \frac{N^T(\ell-1)\ell(\ell+1)(\ell+2)}{2\pi}\int_0^\infty du\frac{j_\ell^2(u)}{u^5} \\ &= \frac{N^T}{15\pi}\frac{1}{(\ell+3)(\ell-2)}, \quad \ell > 2, \end{aligned} \tag{20}$$

in an analogous way as C_ℓ^S in Eq. (6), where the normalization factor N^T is now related to the amplitude A^T in Eq. (2), analogously as N^S for the scalar modes.

Similarly, and following the arguments given in Sec. IV, we will assume that two lower cutoffs equally apply to the integral in Eq. (20) such that

$$\begin{aligned} C^T_{\ell_{\text{odd/even}}} &= N^T\frac{(\ell-1)\ell(\ell+1)(\ell+2)}{2\pi} \\ &\quad\times\int_{u_{\text{min}}^{\text{odd/even}}(\text{tensor})}^{\infty} du\frac{j_\ell^2(u)}{u^5}, \end{aligned} \tag{21}$$

again distinguishing odd from even modes with different lower cutoffs satisfying the ratio $u_{\text{min}}^{\text{even}}(\text{tensor}) = 2u_{\text{min}}^{\text{odd}}(\text{tensor})$.

VII. PARITY STATISTIC ANALYSIS

As mentioned in the Introduction, a possible connection between an "odd universe" (i.e., parity breaking) and the lack for large-angle correlations has been contemplated in the literature, though without a clear theoretical explanation yet (see, e.g., Refs. [29–32]). The deviation from an even-odd parity balance in angular correlations can be studied by means of the parity statistic defined in Refs. [8,9],

$$Q(\ell_{\max}^{\mathrm{odd}}) = \frac{2}{\ell_{\max}^{\mathrm{odd}} - 1} \sum_{\ell=3}^{\ell_{\max}^{\mathrm{odd}}} \frac{D_{\ell-1}}{D_\ell}; \quad \ell_{\max}^{\mathrm{odd}} \geq 3, \tag{22}$$

where $\ell_{\max}^{\mathrm{odd}}$ stands for the maximum odd multipole up to which the statistic is computed. Any deviation from unity of $Q(\ell_{\max}^{\mathrm{odd}})$ as a function of $\ell_{\max}^{\mathrm{odd}}$ points to an even-odd parity imbalance: below unity, it implies odd-parity dominance and a downward tail at large angle in the $C(\theta)$ plot; above 1, it implies even-parity preference and an upward tail. As we shall see soon, the parity statistic $Q(\ell_{\max}^{\mathrm{odd}})$ plays a crucial role in our work assessing the different contributions of scalar and tensor modes to the angular correlations.

A. Physical scale of the infrared cutoffs

From our previous fits to Planck 2018 data in Secs. III and IV, the resulting scalar infrared cutoffs (as comoving wave numbers) turned out to be of order

$$k_{\min} \simeq \frac{\mathrm{few}}{r_d} \approx \mathrm{few} \times 10^{-4}\ \mathrm{Mpc}^{-1}$$
$$\to k_{\min} \simeq \mathrm{few} \times 10^{-42}\ \mathrm{GeV}, \tag{23}$$

where the last figure is expressed in GeV units, which amounts to a very low value indeed. However, physical cutoffs have to be obtained by dividing them by the scale factor, in particular, at the time when compactification of the extra dimension took place (t_{extra}), likely at the very early Universe. Therefore, the corresponding physical wave number, basically set by the inverse radius of the (circular) extra dimension, has to be computed as $k_{\min}/a(t_{\mathrm{extra}})$.

Assuming that the time of compactification happened at some time between the end of the Planck epoch t_{Planck} and the beginning of inflation t_{init}, the respective scale factors $a(t_{\mathrm{Planck}}) \simeq 10^{-61}$ and $a(t_{\mathrm{init}}) \simeq 10^{-56}$ given in [58] lead to the following physical cutoff range:

$$\frac{k_{\min}}{a(t_{\mathrm{extra}})} \in 10^{19} - 10^{14}\ \mathrm{GeV}, \qquad t_{\mathrm{Planck}} < t_{\mathrm{extra}} < t_{\mathrm{init}}, \tag{24}$$

which contains the grand unified theory scale.

Thus, the existence of an infrared cutoff in the CMB temperature correlations is consistent with the assumption of an extra dimension with a high compactification scale.

VIII. FINAL ANALYSIS

Under the arguments given in Sec. IV based on a KK model, the following hierarchy for scalar and tensor lower cutoffs is assumed:

$$u_{\min}^{\mathrm{odd}}(\mathrm{tensor}) = 2u_{\min}^{\mathrm{odd}}(\mathrm{scalar}) = u_{\min}^{\mathrm{even}}(\mathrm{scalar})$$
$$= u_{\min}^{\mathrm{even}}(\mathrm{tensor})/2. \tag{25}$$

Thus, incorporating the tensor contribution in our analysis actually does not mean increasing the number of free fit parameters, except for the extra normalization factor N^T, in Eq. (21). A caveat must be stated: all our following conclusions depend on this closure relation. Let us stress, however, that, from our scan of all other possible values of the lower cutoffs, we can conclude that this particular hierarchy provides the best fits (within the big uncertainties of course) to data points analyzed in this work.

To this end, let us first summarize the successive steps made in this work concerning the set of infrared cutoffs affecting the scalar and tensor power spectra in order to improve the $\chi^2_{\mathrm{d.o.f.}}$ of the fits to the Planck 2018 data points.

(a) No infrared cutoff is introduced to the scalar power spectrum, and the multipole coefficients satisfy the SW plateau, i.e., $C_\ell \sim 1/\ell(\ell+1)$, $\ell \lesssim 30$.
(b) A single infrared cutoff $k_{\min}$ is introduced to the scalar power spectrum corresponding to $u_{\min} = 4.5$ in the integral in Eq. (7).
(c) Two infrared cutoffs $k_{\min}^{\mathrm{odd/even}}$ are introduced to the scalar power spectrum yielding two lower cutoffs $u_{\min}^{\mathrm{even}} = 2u_{\min}^{\mathrm{odd}} \simeq 5.4$ in the integral in Eq. (19).
(d) A set of infrared cutoffs $k_{\min}^{\mathrm{odd/even}}(\mathrm{tensor})$ are further applied to the tensor power spectrum, in addition to the scalar modes, according to the pattern: $u_{\min}^{\mathrm{even}}(\mathrm{tensor}) = 2u_{\min}^{\mathrm{odd}}(\mathrm{tensor})$, as theoretically motivated in Sec. IV.

From the above fits the value of the lower cutoff $u_{\min}^{\mathrm{odd}}(\mathrm{scalar}) = 2.5 \pm 0.3$ is extracted, while all the other (both scalar and tensor) lower cutoffs are determined by the pattern associated with the compact extra dimension, i.e., multiplicative factors 2 relating successive both scaler and tensor $u_{\min}^{\mathrm{odd}}$ and $u_{\min}^{\mathrm{even}}$ following Eq. (25). Note that the value of $u_{\min}^{\mathrm{odd}}(\mathrm{scalar})$ is slightly smaller (but compatible within errors) than the value obtained in Ref. [24] without tensor modes.

Notice that, in addition to the rather modest improvement of the $\chi^2_{\mathrm{d.o.f.}}$ of the fits in Fig. 1 as new cutoffs are incorporated, the downward tail at large angles is only reproduced in cases (c) and (d), where the odd-parity preference can be traced back to the set of infrared cutoffs. More clearly, Fig. 2 shows the increasing improvement of the fits as extra cutoffs are successively incorporated to the fit, reaching $\chi^2_{\mathrm{d.o.f.}} \simeq 0.7$ in case (d), corresponding to a p-value ≃0.9. It is also interesting to note that the inclusion of tensor modes improves the agreement of the expectation curve and $Q\ell_{\max}$ points, especially in the interval $10 \lesssim \ell \lesssim 30$. This remark constitutes a nontrivial result with possible consequences, e.g., for effects on CMB polarization not addressed in this work.

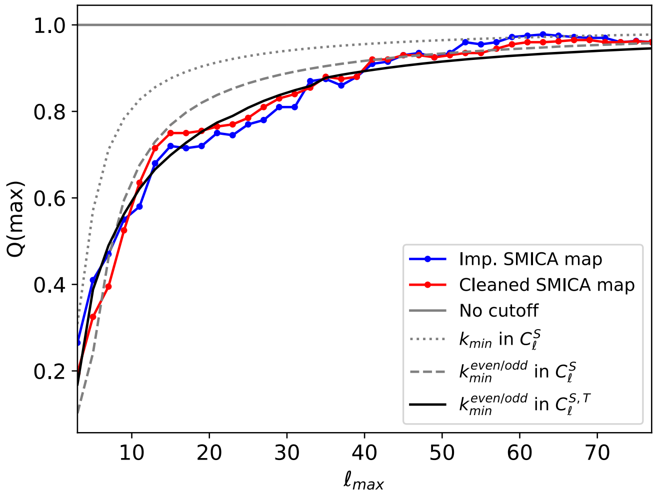

FIG. 2. Parity statistic $Q(\ell_{\mathrm{max}})$ versus ℓ_{max} under the same conditions as in the caption of Fig. 1, and the measured points by Planck (red and blue) under application of two different Spectral Matching Independent Component Analysis (SMICA) masks to suppress undesired foreground.

IX. SUMMARY AND DISCUSSION

We have examined angular temperature correlations of the CMB, following the trail of previous works [24,34,38]. We first introduced a couple of infrared cutoffs into the scalar power spectrum, thereby modifying the behavior of the two-point correlation function $C(\theta)$ and the parity statistic $Q(\ell_{\mathrm{max}})$. In this way we were able to bring the model expectations closer to the Planck 2018 data points. However, the effect on correlations and parity balance is limited to rather low multipoles as $\ell \lesssim 6$ and the improvement finally achieved is rather modest.

Thus, in order to further improve the fits of both $C(\theta)$ and $Q(\ell_{\mathrm{max}})$, tensor modes contributing to the CMB temperature fluctuations were included in the analysis. Let us note that the possibility of unraveling the influence of the cosmological gravitational background on the observed lack of large-angle temperature correlations in the CMB has been envisaged elsewhere, e.g., [59].

On the other hand, motivated by an extra dimension KK model, two sets of infrared cutoffs satisfying $k_{\mathrm{min}}^{\mathrm{even}} = 2k_{\mathrm{min}}^{\mathrm{odd}}$ were introduced to both the scalar and tensor power spectra. The resulting lower cutoffs $u_{\mathrm{min}}^{\mathrm{odd/even}}$ affect differently the $C_{\ell_{\mathrm{odd/even}}}^{S,T}$ coefficients in the Legendre polynomial expansion of $C(\theta)$, consequently modifying the fits to angular distributions. The value of $\chi^2_{\mathrm{d.o.f.}}$ for the $C(\theta)$ fit goes from 2.5 [case (a)] to 0.95 [case(b)], a substantial improvement with respect to the initial assumption of no cutoff at all. Furthermore, the accordance of the parity statistic $Q(\ell_{\mathrm{max}})$ to data largely improves, as can be seen in Fig. 2, reaching $\chi^2_{\mathrm{d.o.f.}} \simeq 0.7$.

Finally, from our analysis we estimate the value of the tensor-to-scalar ratio r defined in Eq. (3). To do so, we employed the ratio C_ℓ^T/C_ℓ^S for different (low) ℓ's computed from our fits of the correlation function $C(\theta)$. The following expression (from [57]) was used:

$$r \approx 0.68 \times \frac{C_\ell^T}{C_\ell^S}. \tag{26}$$

Inserting now the average value $\langle C_\ell^T/C_\ell^S \rangle \simeq 0.04$ computed from our fits over the $10 \leq \ell \leq 20$ interval (where the SW plateau should arise for both scalar and tensor modes), we get the estimate

$$r \simeq 0.027 \pm 0.003, \tag{27}$$

which lies under current limits [25]. Let us point out that the above error bar has been estimated exclusively from the dispersion of the C_ℓ^T/C_ℓ^S values obtained from our fits, while other no less important uncertainties, like the theoretical approximations and modeling dependence used throughout this paper, have not been taken into account. Therefore, the above r value is intended as a consistency test of our results and not a precise determination in this study. We can also cast the above result into usual slow-roll inflation parameters. For example, using $r = 16\epsilon$, we get $\epsilon \simeq 0.0017$, within the slow-roll regime.

As a final remark, uncertainties including the cosmic variance (not considered in this paper), a possible statistical fluke at large angles, contamination or noncosmological effects [33,60], or even alternative theoretical explanations [61] must certainly be kept in mind. Nevertheless, the suggestive accordance achieved between the observed points and fits, when successive sets of infrared cutoffs are incorporated into the scalar and tensor power spectra, is remarkable enough to stress this way of unraveling tensor modes (from PGWs produced during inflation) showing up in CMB temperature correlations, besides the usual search based on the B-mode polarization. In particular, let us point out that the study of cross-power spectra between, e.g., temperature and B modes would provide a crucial information [62]: a non-null signal (contrary to what is expected from the cosmological principle [63,64]) would imply a certain degree of parity breaking (such as odd-parity dominance), which plays a fundamental role in this paper.

ACKNOWLEDGMENTS

M. A. S. L. is thankful for interesting discussions with F. Melia, S. Scopel, D. G. Figueroa, and M. López-Corredoira. M. A. S. L. acknowledges support by the Spanish Agencia Estatal de Investigacion under Grant No. PID2020–113334 GB-I00/AEI/ and by Generalitat Valenciana under Grant No. CIPROM/2022/36. The research of V. S. is supported by the Generalitat Valenciana PROMETEO/2021/083 and the Ministerio de Ciencia e Innovacion PID2020-113644-GB-I00.

APPENDIX: EVEN VERSUS ODD POLYNOMIALS AND CHEBYSHEV POLYNOMIALS

The following relations between Legendre polynomials and the square of cosine functions with entire and half-entire (2π) periods are satisfied, playing a fundamental role in the assignments of the infrared cutoffs to even and odd multipoles in the Legendre expansion of the correlation function $C(\theta)$ [24]:

$$\begin{aligned} P_1(\cos\theta) &= -1 + 2\cos^2(\theta/2), \\ P_2(\cos\theta) &= -0.5 + 1.5\cos^2(\theta), \\ P_3(\cos\theta) &= -1 + 0.75\cos^2(\theta/2) + 1.25\cos^2(3\theta/2), \\ P_4(\cos\theta) &= -0.7184 + 0.6249\cos^2(\theta) + 1.0937\cos^2(2\theta), \\ P_5(\cos\theta) &= -1 + 0.4687\cos^2(\theta/2) + 0.5469\cos^2(3\theta/2) + 0.9844\cos^2(5\theta/2)\cdots. \end{aligned} \tag{A1}$$

Higher-order Legendre polynomials replicate the same pattern: even and odd Legendre polynomials either contain $\cos^2[n\theta]$ or $\cos^2[(n+1/2)\theta]$ terms, to be put in correspondence with the integer and half-integer modes in the Fourier decomposition of the fluctuating field under cyclic conditions.

Alternatively, the above relations can be written in terms of Chebyshev polynomials $T_n(\cos(\theta)) = \cos(n\theta)$ [65], showing again the relationship between the parity of Legendre polynomials and the even/odd cutoffs to compute the coefficients $C_{\ell_{\mathrm{even/odd}}}$,

$$\begin{aligned} P_1(\cos\theta) &= T_1, \\ P_2(\cos\theta) &= 0.25 + 0.75T_2, \\ P_3(\cos\theta) &= 0.375T_1 + 0.625T_3, \\ P_4(\cos\theta) &= 0.1409 + 0.3124T_2 + 0.5468T_4\cdots. \end{aligned} \tag{A2}$$

[1] F. Melia, Tensor fluctuations in the early Universe, Astropart. Phys. **152**, 102876 (2023).
[2] C. Caprini and D. G. Figueroa, Cosmological backgrounds of gravitational waves, Classical Quantum Gravity **35**, 163001 (2018).
[3] C. Chiocchetta, A. Gruppuso, M. Lattanzi, P. Natoli, and L. Pagano, Lack-of-correlation anomaly in CMB large scale polarisation maps, J. Cosmol. Astropart. Phys. 08 (2021) 015.
[4] C. Armitage-Caplan, M. Avillez, D. Barbosa, A. Banday, N. Bartolo, R. Battye, J. P. Bernard, P. de Bernardis, S. Basak, M. Bersanelli *et al.* (COrE Collaboration), COrE (Cosmic origins explorer) a white paper, arXiv:1102.2181.
[5] K. Young, M. Alvarez, N. Battaglia, J. Bock, J. Borrill, D. Chuss, B. Crill, J. Delabrouille, M. Devlin, L. Fissel *et al.*, [NASA PICO] PICO: Probe of inflation and cosmic origins, arXiv:1902.10541.
[6] J. Errard; S. M. Feeney, H. V. Peiris, and A. H. Jaffe, Robust forecasts on fundamental physics from the foreground-obscured, gravitationally-lensed CMB polarization, J. Cosmol. Astropart. Phys. 03 (2016) 052.
[7] C. J. Copi, D. Huterer, D. J. Schwarz, and G. D Starkman, Large angle anomalies in the CMB, Adv. Astron. 847541 (2010).
[8] P. K. Aluri and P. Jain, Parity asymmetry in the CMBR temperature power spectrum, Mon. Not. R. Astron. Soc. **419**, 3378 (2012).
[9] S. Panda, P. K. Aluri, P. K. Samal, and P. K. Rath, Parity in Planck full-mission CMB temperature maps, Astropart. Phys. **125**, 102493 2021.
[10] G. Hinshaw, A. J. Banday, C. L. Bennett, K. M. Górski, A. Kogut, C. H. Lineweaver, and E. L. Wright, 2-point correlations in the COBE DMR four-year anisotropy maps, Astrophys. J. **464**, L25 (1996).
[11] C. L. Bennett, D. Larson, J. L. Weiland, N. Jarosik, G. Hinshaw, N. Odegard, and E. L. Wright, First-Year Wilkinson Microwave Anisotropy Probe (WMAP) observations: Preliminary maps and basic results, Astrophys. J. Suppl. Ser. **148**, 97 (2003).
[12] N. Aghanim, Y. Akrami, M. Ashdown, J. Aumont, C. Baccigalupi, M. Ballardini, and G. Roudier, Planck 2018 results. VI. Cosmological parameters, Astron. Astrophys. **641**, A86 (2018).
[13] Y. Akrami, M. Ashdown, J. Aumont, C. Baccigalupi, M. Ballardini, A. J. Banday, and A. Zonca, Planck 2018 results. VII. Isotropy and statistics of the CMB, Astron. Astrophys. **641**, A7 (2019).
[14] E. Abdalla, G. F. Abellan, A. Aboubrahim, A. Agnello, O. Akarsu, Y. Akrami, and V. Pettorino, Cosmology intertwined: A review of the particle physics, astrophysics, and cosmology associated with the cosmological tensions and anomalies, J. High Energy Astrophys. **34**, 49 (2022).
[15] E. Di Valentino, O. Mena, S. Pan, L. Visinelli, W. Yang, A. Melchiorri, D. F. Mota, A. G. Riess, and J. Silk, In the realm

of the Hubble tension: A review of solutions, Classical Quantum Gravity **38**, 153001 (2021).
[16] S. Shaikh, S. Mukherjee, S. Das, B. Wandelt, and T. Souradeep, Bayesian analysis of large angular scale CMB temperature anomalies, J. Cosmol. Astropart. Phys. 08 (2019) 007.
[17] J. Muir, S. Adhikari, and D. Huterer, Covariance of CMB anomalies, Phys. Rev. D **98**, 023521 (2018).
[18] A. Rassat, J.-L. Starck, P. Paykari, F. Sureau, and J. Bobin, Planck CMB anomalies: Astrophysical and cosmological secondary effects and the curse of masking, J. Cosmol. Astropart. Phys. 08 (2014) 006.
[19] M. Thomson, *Modern Particle Physics* (Cambridge University Press, Cambridge, England, 2013).
[20] A. Lue, L. M. Wang, and M. Kamionkowski, Cosmological signature of new parity violating interactions, Phys. Rev. Lett. **83**, 1506 (1999).
[21] M. Satoh, S. Kanno, and J. Soda, Circular polarization of primordial gravitational waves in string-inspired inflationary cosmology, Phys. Rev. D **77**, 023526 (2008).
[22] S. Alexander and N. Yunes, Chern-Simons modified general relativity, Phys. Rep. **480**, 1 (2009).
[23] J. Qiao, Z. Li, T. Zhu. R. Ji, G. Li, and W. Zao, Testing parity symmetry of gravity with gravitational waves, Front. Astron. Space Sci. **9**, 1109086 (2023).
[24] M. A. Sanchis-Lozano, Stringy signals from large-angle correlations in the cosmic microwave background?, Universe **8**, 396 (2022).
[25] R. L. Workman *et al.* (Particle Data Group), Review of particle physics, Prog. Theor. Exp. Phys. **8**, 083C01 (2022).
[26] E. W. Kolb and M. Turner, *The Early Universe, Frontiers in Physics* (Westview Press, Boulder, CO, 1994).
[27] A. Gangui, F. Lucchin, S. Matarrese, and S. Mollerach, The three-point correlation function of the cosmic microwave background in inflationary models, Astrophys. J. **430**, 447 (1994).
[28] M. Kamionkowski and T. Souradeep, The odd-parity CMB bispectrum, Phys. Rev. D **83**, 027301 (2011).
[29] K. Land and J. Magueijo, Is the Universe odd?, Phys. Rev. D **72**, 101302 (2005).
[30] J. Kim, P. Naselsky, and M. Hansen, Symmetry and antisymmetry of the CMB anisotropy pattern, Adv. Astron. 960509 (2012).
[31] D. J. Schwarz, C. J. Copi, D. Huterer, and G. D. Starkman, CMB anomalies after Planck, Classical Quantum Gravity **33**, 184001 (2016).
[32] C. J. Copi, J. Gurian, A. Kosowsky, G. D. Starkman, and H Zhang, Exploring suppressed long-distance correlations as the cause of suppressed large-angle correlations, Mon. Not. R. Astron. Soc. **490**, 1 (2018).
[33] W. Zhao and L. Santos, Preferred axis in cosmology, Universe **3**, 9 (2015).
[34] F. Melia and M. López-Corredoira, Evidence of a truncated spectrum in the angular correlation function of the cosmic microwave background, Astron. Astrophys. **610**, A87 (2018).
[35] F. Melia, Quantum fluctuations at the Planck scale, Eur. Phys. J. C **79**, 455 (2019).
[36] F. Melia, Angular correlation of the CMB in the $R_h = ct$ universe, Astron. Astrophys. **561**, A80 (2012).
[37] F. Melia, Q. Ma, J. J. Wei, and B. Yu, Hint of a truncated primordial spectrum from the CMB large-scale anomalies, Astron. Astrophys. **655**, A70 (2021).
[38] M. A. Sanchis-Lozano, F. Melia, M. Lopez-Corredoira, and N. Sanchis-Gual, Missing large-angle correlations versus odd-parity dominance in the cosmic microwave background, Astron. Astrophys. **10**, 142 (2022).
[39] D. Samart, C. Pongkitivanichkul, and P. Channuie, Composite dynamics and cosmology: Inflation, Eur. Phys. J. Special Topics **231**, 1325 (2022).
[40] J. G. Lee, E. G. Adelberger, T. S. Cook, S. M. Fleischer, and B. R. Heckel, New test of the gravitational $1/r^2$ law at separations down to 52 μm, Phys. Rev. Lett. **124**, 101101 (2020).
[41] R. Fok, C. Guimaraes, R. Lewis, and V. Sanz, It is a graviton! Or maybe not, J. High Energy Phys. 12 (2012) 062.
[42] J. M. Maldacena, The large *N* limit of superconformal field theories and supergravity, Adv. Theor. Math. Phys. **2**, 231 (1998).
[43] J. Hirn and V. Sanz, Interpolating between low and high energy QCD via a 5-D Yang-Mills model, J. High Energy Phys. 12 (2005) 030.
[44] A. Donini, V. Enguita-Vileta, F. Esser, and V. Sanz, Generalising holographic superconductors, Adv. High Energy Phys. **2022**, 1785050 (2022).
[45] J. Hirn and V. Sanz, A negative *s* parameter from holographic technicolor, Phys. Rev. Lett. **97**, 121803 (2006).
[46] J. Hirn and V. Sanz, The fifth dimension as an analog computer for strong interactions at the LHC, J. High Energy Phys. 03 (2007) 100.
[47] D. Croon and V. Sanz, Saving natural inflation, J. Cosmol. Astropart. Phys. 02 (2005) 008.
[48] T. Sakai and S. Sugimoto, Low energy hadron physics in holographic QCD, Prog. Theor. Phys. **113**, 843 (2005).
[49] J. Hirn, N. Rius, and V. Sanz, Geometric approach to condensates in holographic QCD, Phys. Rev. D **73**, 085005 (2006).
[50] A. Karch, E. Katz, D. T. Son, and M. A. Stephanov, Linear confinement and AdS/QCD, Phys. Rev. D **74**, 015005 (2006).
[51] J. Hirn and V. Sanz, (Not) summing over Kaluza-Kleins, Phys. Rev. D **76**, 044022 (2007).
[52] K. w. Choi and I. W. Kim, One loop gauge couplings in AdS (5), Phys. Rev. D **67**, 045005 (2003).
[53] B. M. Dillon and V. Sanz, Kaluza-Klein gravitons at LHC2, Phys. Rev. D **96**, 035008 (2017).
[54] L. Campanelli, P. Cea, and L. Tedesco, Ellipsoidal universe can solve the CMB quadrupole problem, Phys. Rev. Lett. **97**, 131202 (2006); **97**, 209903(E) (2006).
[55] L. Campanelli, P. Cea, and L. Tedesco, Cosmic microwave background quadrupole and ellipsoidal universe, Phys. Rev. D **76**, 063007 (2007).
[56] P. Cea, CMB 2-point angular correlation function in the ellipsoidal universe, Int. J. Mod. Phys. A **38**, 2350030 (2023).
[57] V. F. Mukhanov, *Physical Foundations of Cosmology* (Cambridge University Press, Cambridge, United Kingdom, 2005).
[58] J. Liu and F. Melia, Inflation with self-consistent initial conditions (to be published).

[59] G. Galloni, M. Ballardini, N. Bartolo, A. Gruppuso, L. Pagano, and A. Ricciardone, Unraveling the CMB lack-of-correlation anomaly with the cosmological gravitational wave background, J. Cosmol. Astropart. Phys. 10 (2023) 013.

[60] J. Creswell and P. Naselsky, Asymmetry of the CMB map: Local and global anomalies, J. Cosmol. Astropart. Phys. 03 (2021) 103.

[61] A. Ashtekar, B. Gupt, D. Jeong, and V. Sreenath, Alleviating the tension in the cosmic microwave background using Planck-scale physics, Phys. Rev. Lett. **125**, 051302 (2020).

[62] J. Chen, S. Ghosh, and W. Zhao, Scalar quadratic maximum-likelihood estimators for the CMB cross-power spectrum, Astrophys. J. Suppl. Ser. **260**, 44 (2022).

[63] L. M. Krauss, S. Dodelson, and S. Meyer, Primordial gravitational waves and cosmology, Science **328**, 989 (2010).

[64] J. Garcia-Bellido, Primordial gravitational waves from inflation and preheating, Prog. Theor. Phys. Suppl. **190**, 322 (2011).

[65] M. Abramowitz and I. A. Segun, *Handbook of Mathematical Functions: With Formulas, Graphs and Mathematical Tables* (Dover Publications, New York, 1970).